annual availability function after a single, new machine is added, assuming that nothing else is altered. Let

| | |
|---|---|
| $C$ | capacity of new machine, MW |
| $A(M)$ | annual availability of the basic system as a function of the margin $M$ |
| $M$ | reserve margin |
| $a$ | availability of the new machine. |

Thus, the new availability function becomes

$$A'(M) = aA(M - C) + (1 - a)A(M). \quad (33)$$

This relationship may be used to consider the effect of adding different machine capacities on the annual availability (i.e., the loss-of-load probability). A similar relationship may be worked out for the frequency calculations. These are approximate since they assume no change in maintenance outages for the old machines and that the new machine is not maintained during the year.

The technique for constructing the load model suggested by Mr. Adler is similar to that used by the authors and their associates. That is, historical load data are examined statistically to establish periodic (i.e., monthly or seasonal), per unit peak load variation curves, and monthly or seasonal peaks in per unit of the annual peak. The data requirements are then primarily for the annual peak load forecasts. It might be observed that the load model of the paper does not require that the occurrence $N$ of a load level of $L_i$ MW be an integer value. This might be useful in specifying the peak load variation curve from historical data since, for instance, a model for a 30-day period might include 35 load levels. This would permit using more data to define the highest load levels in the peak variation curve. The load model also requires the specification of the mean duration $e$ of the peak periods. This value is a matter of judgment, to be arrived at after a suitable study of load cycle data. Values of from 1/4 to over 1/2 of a day would seem to be appropriate for various different systems.

Concerning Mr. Watchorn's question about representing hydro units and plants (energy limits and head effects), we have not included these provisions in the analysis. However, we would like to note that the frequency and duration method will handle the same problems that may be treated by loss-of-load probability.

We agree with Mr. Watchorn that the "economic criterion" would be "by far the most meaningful aid to judgment." Even separate economic criteria for bulk power supply and for distribution systems would be of much value for system planning.

Again we wish to thank the various discussers for their contributions. It is gratifying to observe the continuing interest in this area.

# Digital Computer Solution of Electromagnetic Transients in Single- and Multiphase Networks

HERMANN W. DOMMEL, MEMBER, IEEE

*Abstract*—**Electromagnetic transients in arbitrary single- or multiphase networks are solved by a nodal admittance matrix method. The formulation is based on the method of characteristics for distributed parameters and the trapezoidal rule of integration for lumped parameters. Optimally ordered triangular factorization with sparsity techniques is used in the solution. Examples and programming details illustrate the practicality of the method.**

## I. Introduction

THIS PAPER describes a general solution method for finding the time responses of electromagnetic transients in arbitrary single- or multiphase networks with lumped and distributed parameters. A computer program based on this method has been used at the Bonneville Power Administration (BPA) and the Munich Institute of Technology, Germany, for analyzing transients in power systems and electronic circuits [1], [2]. Among the useful features of this program are the inclusion of nonlinearities, any number of switchings during the transient in accordance with specified switching criteria, start from any nonzero initial condition, and great flexibility in specifying voltage and current excitations of various waveforms.

The digital computer cannot give a continuous history of the transient phenomena, but rather a sequence of snapshot pictures at discrete intervals $\Delta t$. Such discretization causes truncation errors which can lead to numerical instability [3]. For this reason the trapezoidal rule was chosen for integrating the ordinary differential equations of lumped inductances and capacitances; it is simple, numerically stable, and accurate enough for practical purposes.

Branches with distributed parameters are assumed to be lossless; they will be called lossless lines hereafter. By neglecting the losses (which can be approximated very accurately in other ways, as will be shown) an exact solution can be obtained with the method of characteristics. This method has primarily been used in Europe, where it is known as Bergeron's method; it was first applied to hydraulic problems in 1928 and later to electrical problems (for historic notes see [5]). It is well suited for digital computers [6]–[8]. In contrast to the alternative lattice method for traveling wave phenomena [9] it offers important advantages; for example, no reflection coefficients are necessary when this method is used.

Paper 68 TP 657-PWR, recommended and approved by the Power System Engineering Committee of the IEEE Power Group for presentation at the IEEE Summer Power Meeting, Chicago, Ill., June 23–28, 1968. Manuscript submitted February 12, 1968; made available for printing April 10, 1968. The early stages of this work were sponsored by the German Research Association (Deutsche Forschungsgemeinschaft) while the author was with the Munich Institute of Technology.

The author is with Bonneville Power Administration, Portland, Ore.

The method of characteristics and the trapezoidal rule can easily be combined into a generalized algorithm capable of solving transients in any network with distributed as well as lumped parameters. Numerically this leads to the solution of a system of linear (nodal) equations in each time step. It will be shown that lossless lines contribute only to the diagonal elements of the associated matrix; off-diagonal elements result only from lumped parameters. Thus a very fast and simple algorithm can be written when lumped parameters are excluded. However, no such restrictions are imposed. Instead, the recent impressive advances in solving linear equations by sparsity techniques and optimally ordered elimination [10] have been incorporated into an algorithm which automatically encompasses the fast solution of the restricted case and yet retains full generality.

## II. Solution for Single-Phase Networks

A digital computer solution for transients is necessarily a step-by-step procedure that proceeds along the time axis with a variable or fixed step width $\Delta t$. The latter is assumed here. Starting from initial conditions at $t = 0$, the state of the system is found at $t = \Delta t, 2\Delta t, 3\Delta t, \ldots$, until the maximum time $t_{max}$ for the particular case has been reached. While solving for the state at $t$, the previous states at $t - \Delta t, t - 2\Delta t, \ldots$, are known. A limited portion of this "past history" is needed in the method of characteristics, which is used for lines, and in the trapezoidal rule of integration, which is used for lumped parameters. In the first case it must date back over a time span equal to the travel time of the line; in the latter case, only to the previous step. With a record of this past history, the equations of both methods can be represented by simple equivalent impedance networks. A nodal formulation of the problem is then derived from these networks.

### *Lossless Line*

Although the method of characteristics is applicable to lossy lines, the ordinary differential equations which it produces are not directly integrable [8]. Therefore, losses will be neglected at this stage. Consider a lossless line with inductance $L'$ and capacitance $C'$ per unit length. Then at a point $x$ along the line voltage and current are related by

$$-\partial e/\partial x = L'(\partial i/\partial t) \tag{1a}$$

$$-\partial i/\partial x = C'(\partial e/\partial t). \tag{1b}$$

The general solution, first given by d'Alembert, is

$$i(x, t) = f_1(x - vt) + f_2(x + vt) \tag{2a}$$

$$e(x, t) = Z \cdot f_1(x - vt) - Z \cdot f_2(x + vt) \tag{2b}$$

with $f_1(x - vt)$ and $f_2(x + vt)$ being arbitrary functions of the variables $(x - vt)$ and $(x + vt)$. The physical interpretation of $f_1(x - vt)$ is a wave traveling at velocity $v$ in a forward direction and of $f_2(x + vt)$ a wave traveling in a backward direction. $Z$ in (2) is the surge impedance, $v$ is the phase velocity

$$Z = \sqrt{L'/C'} \tag{3a}$$

$$v = 1/\sqrt{L'C'}. \tag{3b}$$

Multiplying (2a) by $Z$ and adding it to or subtracting it from (2b) gives

$$e(x, t) + Z \cdot i(x, t) = 2Z \cdot f_1(x - vt) \tag{4}$$

$$e(x, t) - Z \cdot i(x, t) = -2Z \cdot f_2(x + vt). \tag{5}$$

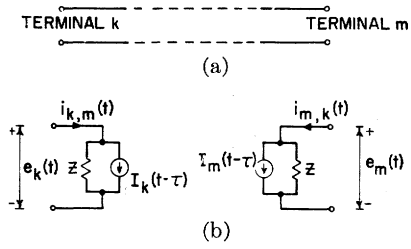


Fig. 1. (a) Lossless line. (b) Equivalent impedance network.

Note that in (4) the expression $(e + Zi)$ is constant when $(x - vt)$ is constant and in (5) $(e - Zi)$ is constant when $(x + vt)$ is constant. The expressions $(x - vt) =$ constant and $(x + vt) =$ constant are called the characteristics of the differential equations.

The significance of (4) may be visualized in the following way: let a fictitious observer travel along the line in a forward direction at velocity $v$. Then $(x - vt)$ and consequently $(e + Zi)$ along the line will be constant for him. If the travel time to get from one end of the line to the other is

$$\tau = d/v = d\sqrt{L'C'} \tag{6}$$

($d$ is the length of line), then the expression $(e + Zi)$ encountered by the observer when he leaves node $m$ at time $t - \tau$ must still be the same when he arrives at node $k$ at time $t$, that is

$$e_m(t - \tau) + Zi_{m,k}(t - \tau) = e_k(t) + Z(-i_{k,m}(t))$$

(currents as in Fig. 1). From this equation follows the simple two-port equation for $i_{k,m}$

$$i_{k,m}(t) = (1/Z)e_k(t) + I_k(t - \tau)$$

and analogous (7a)

$$i_{m,k}(t) = (1/Z)e_m(t) + I_m(t - \tau)$$

with equivalent current sources $I_k$ and $I_m$, which are known at state $t$ from the past history at time $t - \tau$,

$$I_k(t - \tau) = -(1/Z)e_m(t - \tau) - i_{m,k}(t - \tau)$$

$$I_m(t - \tau) = -(1/Z)e_k(t - \tau) - i_{k,m}(t - \tau). \tag{7b}$$

Fig. 1 shows the corresponding equivalent impedance network, which fully describes the lossless line at its terminals. Topologically the terminals are not connected; the conditions at the other end are only seen indirectly and with a time delay $\tau$ through the equivalent current sources $I$.

### *Inductance*

For the inductance $L$ of a branch $k, m$ (Fig. 2) we have

$$e_k - e_m = L(di_{k,m}/dt) \tag{8a}$$

which must be integrated from the known state at $t - \Delta t$ to the unknown state at $t$:

$$i_{k,m}(t) = i_{k,m}(t - \Delta t) + \frac{1}{L}\int_{t-\Delta t}^{t} (e_k - e_m)\, dt. \tag{8b}$$

Using the trapezoidal rule of integration yields the branch equation

$$i_{k,m}(t) = (\Delta t/2L)(e_k(t) - e_m(t)) + I_{k,m}(t - \Delta t) \tag{9a}$$

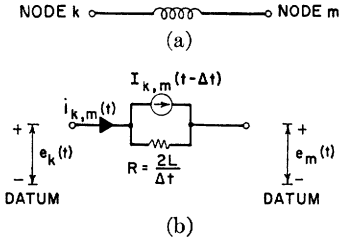


Fig. 2. (a) Inductance. (b) Equivalent impedance network.

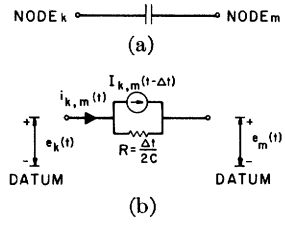


Fig. 3. (a) Capacitance. (b) Equivalent impedance network.

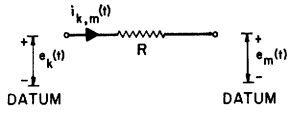


Fig. 4. Resistance.

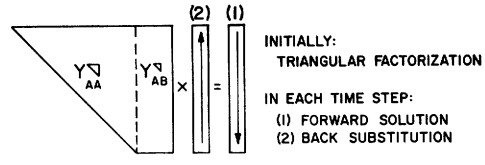


Fig. 5. Repeat solutions of linear equations.

where the equivalent current source $I_{k,m}$ is again known from the past history:

$$I_{k,m}(t-\Delta t) = i_{k,m}(t-\Delta t) + (\Delta t/2L)\,(e_k(t-\Delta t) - e_m(t-\Delta t)). \quad (9b)$$

The discretization with the trapezoidal rule produces a truncation error of order $(\Delta t)^3$; if $\Delta t$ is sufficiently small and cut in half, then the error can be expected to decrease by the factor 1/8. Note that the trapezoidal rule for integrating (8b) is identical with replacing the differential quotient in (8a) by a central difference quotient at midpoint between $(t-\Delta t)$ and $t$ with linear interpolation assumed for $e$. The equivalent impedance network corresponding to (9) is shown in Fig. 2.

*Capacitance*

For the capacitance $C$ of a branch $k, m$ (Fig. 3) the equation

$$e_k(t) - e_m(t) = \frac{1}{C}\int_{t-\Delta t}^{t} i_{k,m}(t)\,dt + e_k(t-\Delta t) - e_m(t-\Delta t)$$

can again be integrated with the trapezoidal rule, which yields

$$i_{k,m}(t) = (2C/\Delta t)\,(e_k(t) - e_m(t)) + I_{k,m}(t-\Delta t) \quad (10a)$$

with the equivalent current source $I_{k,m}$ known from the past history:

$$I_{k,m}(t-\Delta t) = -i_{k,m}(t-\Delta t) - (2C/\Delta t)\,(e_k(t-\Delta t) - e_m(t-\Delta t)). \quad (10b)$$

An equivalent impedance network is shown in Fig. 3. Its form is identical with that for the inductance. The discretization error is also the same as that for the inductance.

*Resistance*

For completeness we add the branch equation for the resistance (Fig. 4):

$$i_{k,m}(t) = (1/R)\,(e_k(t) - e_m(t)). \quad (11)$$

*Nodal Equations*

With all network elements replaced by equivalent impedance networks as in Figs. 1–4, it is very simple to establish the nodal equations for any arbitrary system. The procedures are well known [3] and will not be explained here. The result is a system of linear algebraic equations that describes the state of the system at time $t$:

$$[Y][e(t)] = [i(t)] - [I] \quad (12)$$

with

- $[Y]$ nodal conductance matrix
- $[e(t)]$ column vector of node voltages at time $t$
- $[i(t)]$ column vector of injected node currents at time $t$ (specified current sources from datum to node)
- $[I]$ known column vector, which is made up of known equivalent current sources $I$.

Note that the real symmetric conductance matrix $[Y]$ remains unchanged as long as $\Delta t$ remains unchanged. It is, therefore, preferable, though not mandatory, to work with fixed step width $\Delta t$. The formation of $[Y]$ follows the rules for forming the nodal admittance matrix in steady-state analysis.

In (12) part of the voltages will be known (specified excitations) and the others will be unknown. Let the nodes be subdivided into a subset $A$ of nodes with unknown voltages and a subset $B$ of nodes with known voltages. Subdividing the matrices and vectors accordingly, we get from (12)

$$\begin{bmatrix} [Y_{AA}] & [Y_{AB}] \\ [Y_{BA}] & [Y_{BB}] \end{bmatrix} \begin{bmatrix} [e_A(t)] \\ [e_B(t)] \end{bmatrix} = \begin{bmatrix} [i_A(t)] \\ [i_B(t)] \end{bmatrix} - \begin{bmatrix} [I_A] \\ [I_B] \end{bmatrix}$$

from which the unknown vector $[e_A(t)]$ is found by solving

$$[Y_{AA}][e_A(t)] = [I_{\text{total}}] - [Y_{AB}][e_B(t)] \quad (13)$$

with

$$[I_{\text{total}}] = [i_A(t)] - [I_A].$$

This amounts to the solution of a system of linear equations in each time step with a constant coefficient matrix $[Y_{AA}]$, provided $\Delta t$ is not changed. The right sides in (13) must be recalculated in each time step.

*Practical Computation*

Equation (13) is best solved by triangular factorization of the augmented matrix $[Y_{AA}]$, $[Y_{AB}]$ once and for all before entering the time step loop. The same process is then extended to the vector $[I_{\text{total}}]$ in each time step in the so-called forward solution, followed by back substitution to get $[e_A(t)]$, as indi-

cated in Fig. 5. Only a few elements in $[Y_{AA}]$, $[Y_{AB}]$ are nonzero; this sparsity is exploited by storing only the nonzero elements of the triangularized matrix. The savings in computer time and storage requirements can be optimized with an ordered elimination scheme [10].

Should the nodes be connected exclusively via lossless lines, with lumped parameters $R$, $L$, $C$ only from nodes to datum, then $[Y_{AA}]$ becomes a diagonal matrix. In this case the equations could be solved separately node by node. Some programs are based on this restricted topology. However, the sparsity technique lends itself automatically to this simplification without having to restrict the generality of the network topology.

The construction of the column vector $[I_{\text{total}}]$ is mainly a bookkeeping problem. Excitations in the form of specified current sources $[i_A(t)]$ and the past history information in $-[I_A]$ are entered into $[I_{\text{total}}]$ before going into the forward solution; after $[I_{\text{total}}]$ has been built, using the still available voltages from the previous time step, specified voltage sources $[e_B(t)]$ are entered into $[e(t)]$. Excitation values may be read from cards step-by-step or calculated from standardized functions (sinusoidal curve, rectangular wave[1], etc.). The excitations may be any combination of voltage and current sources, or there may be no excitation at all (e.g., discharge of capacitor banks). After having found $[e_A(t)]$, the past history records are updated while constructing the vector $[I_{\text{total}}]$ for the next time step (see flow chart in Fig. 6). Some practical hints about recording the past history and about nonzero initial conditions may be found in Appendixes I and II.

*Approximation of Series Resistance of Lines*

The simplicity of the method of characteristics rests on the fact that losses are neglected. This simplicity also holds for the distortionless line, where $R'/L' = G'/C'$ ($R'$ is the series resistance and $G'$ the shunt conductance per unit length); the only difference is in computing $I_k$ (and analogous $I_m$):

$$I_k(t-\tau) = \exp(-(R'/L')\tau)\,(-(1/Z)e_m(t-\tau) - i_{m,k}(t-\tau)).$$

Unfortunately, power lines are not distortionless, since $G'$ is usually negligible (or a very complicated function of voltage if corona is to be taken into account).

The distributed series resistance with $G' = 0$ can easily be approximated by treating the line as lossless and adding lumped resistances at both ends. Such lumped resistances can be inserted in many places along the line when the total length is divided into many line sections. Interestingly, all cases tested so far showed no noticeable difference between lumped resistances inserted in few or in many places. The voltage plot in Fig. 13 was practically identical for lumped resistances inserted in 3, 65, and 300 places. In its present form, BPA's program automatically lumps $R/4$ at both ends and $R/2$ at the middle of the line ($R$ is the total series resistance); under these assumptions the equivalent impedance network of Fig. 1 is still valid and only the values change slightly ($I_m$ analogous to $I_k$):

$$Z = \sqrt{L'/C'} + \tfrac{1}{4}R$$

$$I_k(t-\tau) = ((1+h)/2)\{I_k \text{ from eq. (7b)}\} + ((1-h)/2)\{I_m \text{ from eq. (7b)}\}$$

with

$$h = (Z - \tfrac{1}{4}R)/(Z + \tfrac{1}{4}R).$$

The real challenge for a better line representation is the frequency dependence of $R'$ and $L'$, which results from skin effects in the earth return [11] and in the conductors; BPA plans to explore this further (see Section IV).

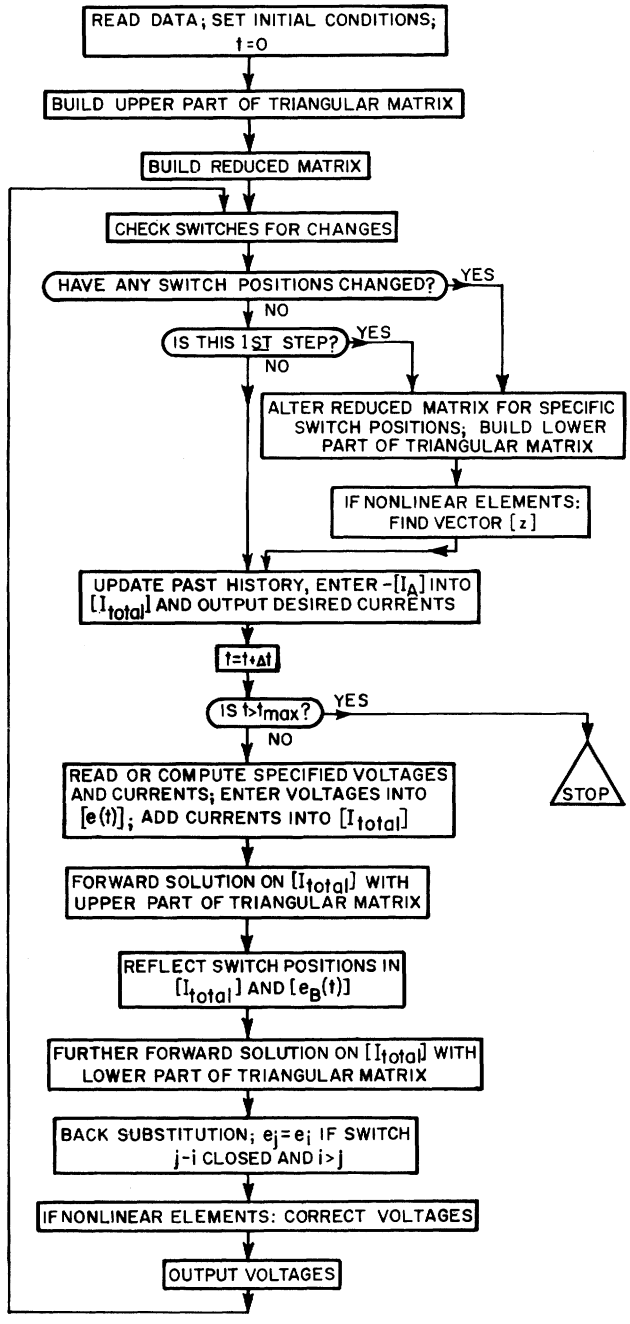


Fig. 6. Flow chart for transients program.

*Switches*

The network may include any number of switches, which may change their positions in accordance with defined criteria. They are represented as ideal ($R = 0$ when closed and $R = \infty$ when open); however, any branches may be connected in series or parallel to simulate physical properties (e.g., time-varying or current-dependent resistance).

[1] Since the trapezoidal rule is based on linear interpolation, a rectangular wave of amplitude $y$ will always be interpreted as having a finite rate of rise $y/\Delta t$ in the first step in the presence of lumped inductances and capacitances.

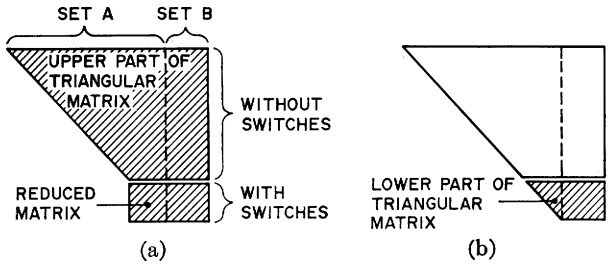


Fig. 7. Shaded areas show computation. (a) Initially. (b) After each change.

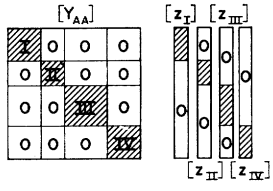


Fig. 9. Disconnected subnetworks in $[Y_{AA}]$.

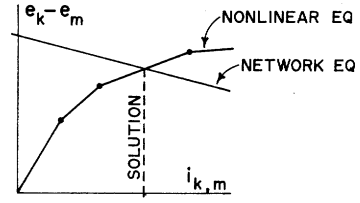


Fig. 8. Solution for nonlinear parameter.

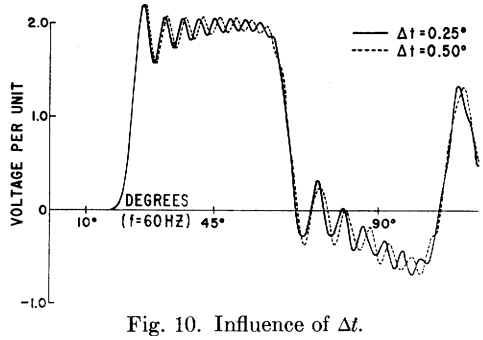


Fig. 10. Influence of $\Delta t$.

With only one switch in the network, it is best to build the matrix for the switch open and to simulate the closed position with superimposed node currents [2]. With more switches in the network, it is preferable to build $[Y_{AA}]$, $[Y_{AB}]$ anew each time a change occurs. However, it is not necessary to repeat the entire triangular factorization with each change. Nodes with switches connected are arranged at the bottom (Fig. 7). Then the triangular factorization is carried out only for nodes without switches (upper part of triangular matrix). This also yields a reduced matrix for the nodes with switches (assumed to be open). Whenever a switch position changes, this reduced matrix is first modified to reflect the actual switch positions (if closed: addition of respective rows and columns and retention of the higher numbered node in place of two nodes), then the triangular factorization is completed (lower part of triangular matrix). This scheme is included in the flow chart of Fig. 6.

*Nonlinear and Time-Varying Parameters*

With only one nonlinear parameter in the network, the solution can be kept essentially linear by confining the nonlinear algorithm (usually an iterative procedure) to the branch with the nonlinear parameter. To accomplish this the nonlinear parameter is not included in the matrix; its current $i_{k,m}$ is simulated with two additional node currents:

$$i_m = i_{k,m} \quad \text{and} \quad i_k = -i_{k,m}.$$

Let $[z]$ be the precalculated difference of the $m$th and $k$th columns of $[Y_{AA}]^{-1}$, which is readily obtained with a repeat solution of (13) by setting $[I_{\text{total}}] = \{0$, except $+1.0$ in $m$th and $-1.0$ in $k$th component$\}$ and $[e_B(t)] = 0$. Ignoring the nonlinear parameter at first, we get $[e_A{}^{(\text{linear})}(t)]$ from (13); the final solution follows from superimposing the two additional currents $i_k = -i_m = -i_{k,m}$:

$$[e_A(t)] = [e_A{}^{(\text{linear})}(t)] + [z] \cdot i_{k,m}(t). \tag{14}$$

The value $i_{k,m}$ in (14) is found by solving two simultaneous equations, the linear network equation (Thévenin equivalent)

$$e_k(t) - e_m(t) = e_k{}^{(\text{linear})}(t) - e_m{}^{(\text{linear})}(t) + (z_k - z_m) \cdot i_{k,m}(t) \tag{15}$$

and the nonlinear equation in the form of the given characteristic,

$$e_k(t) - e_m(t) = f(i_{k,m}(t)). \tag{16a}$$

BPA's program represents the nonlinear characteristic point-by-point as piecewise linear (Fig. 8), but any mathematical function could be used instead.

The nonlinear characteristic (16a) is that of a nonlinear, current-dependent resistance. If it is to represent a lightning arrester, then $i_{k,m} = 0$ until $|e_k{}^{(\text{linear})}(t) - e_m{}^{(\text{linear})}(t)|$ reaches the specified breakdown voltage of the arrester.

For a time-varying resistance, (16a) must be replaced by the simpler equation

$$e_k(t) - e_m(t) = R(t_R) \cdot i_{k,m}(t) \tag{16b}$$

where $R(t_R)$ is given as a function of the time $t_R$ (e.g., in the form of a table). The time count $t_R$ may be identical with the time $t$ of the transient study, or it may start later according to a defined criterion.

The characteristic of a nonlinear inductance is usually specified as $\psi = f(i_{k,m})$. The total flux is

$$\psi(t) = \int_0^t (e_k(t) - e_m(t))\, dt + \psi(0).$$

With the trapezoidal rule of integration this becomes

$$e_k(t) - e_m(t) = (2/\Delta t) f(i_{k,m}(t)) - c(t - \Delta t), \tag{16c}$$

which simply replaces (16a). The value $c$ must be updated with

$$c(0) = (2/\Delta t)\, \psi(0) + e_k(0) - e_m(0)$$

and then recursively

$$c(t - \Delta t) = c(t - 2\Delta t) + 2(e_k(t - \Delta t) - e_m(t - \Delta t)).$$

Generally, when a network contains more than one nonlinear parameter, the entire problem becomes nonlinear and its iterative solution quite lengthy. The algorithm remains simple, however, if the network is topologically disconnected into subnetworks, each containing only one nonlinear parameter. Disconnections give $[Y_{AA}]$ a diagonal structure with submatrices on the diagonal (Fig. 9). Note that topological disconnections are quite likely in networks containing lossless lines, since they, as well as lumped parameters from node to datum or to nodes with known

voltage, do not introduce off-diagonal elements into $[Y_{AA}]$. For each subnetwork there is an independent equation (15) and each vector $[z]$ has zeros outside of that subnetwork. (Fig. 9 symbolizes nonlinear parameters I–IV in four effectively disconnected subnetworks.) Therefore each nonlinear parameter can be treated separately and exactly as above. In the superposition (14), each subnetwork will have its own $[z]$ and $i_{k,m}$. However, it is possible to compress these columns ($[z_I]$–$[z_{IV}]$ in Fig. 9) into one single column, if an address column is added to indicate the number of the subnetwork; the latter is necessary to insert the right current $i_{k,m}$ into (14). BPA's program automatically checks for violations of the disconnection rule while computing this single column together with the address column.

*Accuracy*

To arrive at (13), approximations have to be made only for lumped inductances and capacitances. Lossless lines and resistances are treated rigorously.

In practice, a truncation error is introduced by a lossless line whenever its travel time $\tau$ is not an integer multiple of $\Delta t$. Then some kind of interpolation becomes necessary in computing $I_k(t-\tau)$ and $I_m(t-\tau)$. One option in BPA's program uses linear interpolation, because in most practical cases the curves $e(t)$ and $i(t)$ are smooth rather than discontinuous. For cases with expected discontinuities, another option rounds the travel time $\tau$ to the nearest integer multiple of $\Delta t$. Both options raise travel times $\tau < \Delta t$ to $\Delta t$; otherwise the equivalent impedance network of Fig. 1 could not be used any more.

The trapezoidal rule of integration, used for lumped inductances and capacitances, is considered to be adequate for practical purposes, especially if the network has only a few lumped parameters. Compared with the alternative of stubline approximations [9], the results are more accurate. It is well known that the trapezoidal rule is numerically stable and has almost ideal round-off properties [12, p. 119]. When the step-width $\Delta t$ is chosen sufficiently small to give good curve plots (points not spaced too widely), linear interpolation, on which the trapezoidal rule is based, should be a good approximation. Both requirements go hand in hand. The choice of $\Delta t$ is not critical as long as the oscillations of highest frequency are still represented by an adequate number of points. Changing $\Delta t$ influences primarily the phase position of the high-frequency oscillations; the amplitude remains practically unchanged (see Fig. 10 which resulted from an example similar to that of Fig. 12).

Higher accuracy could be obtained with the Richardson extrapolation [12, p. 118]. Here, the integration from $(t-\Delta t)$ to $t$ would be carried out twice, with $\Delta t$ in one step and with $\Delta t/2$ in two steps, and both results extrapolated to $\Delta t = 0$. The amount of work in each time step is thus tripled and the work for the initial triangular factorization is doubled, since two matrices, built for $\Delta t$ and $\Delta t/2$, are necessary.

## III. Mutual Coupling and Multiphase Networks

*Lumped Parameters with Mutual Coupling*

To include mutual coupling with lumped parameters the scalar quantities of a single branch are simply replaced by matrix quantities for the set of coupled branches. Consider the three coupled branches in Fig. 11 with a resistance matrix $[R]$ and an inductance matrix $[L]$. They could represent the series branches of a three-phase $\pi$-equivalent with earth return; in this case $[L]$ as well as $[R]$ would have off-diagonal elements (mutual coupling). Applying the trapezoidal rule of integration [2] yields:

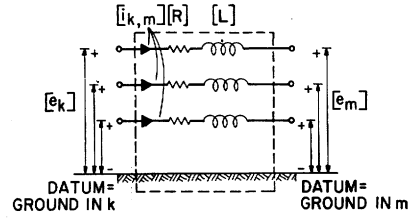


Fig. 11. Mutual coupling.

$$[i_{k,m}(t)] = [S]^{-1}([e_k(t)] - [e_m(t)]) + [I_{k,m}(t-\Delta t)] \quad (17a)$$

with $[I_{k,m}(t-\Delta t)]$ from the recursive formula

$$[I_{k,m}(t-\Delta t)] = [H]([e_k(t-\Delta t)] - [e_m(t-\Delta t)] + [S][I_{k,m}(t-2\Delta t)]) - [I_{k,m}(t-2\Delta t)]. \quad (17b)$$

All matrices in (17) are symmetric:

$$[S] = [R] + (2/\Delta t)[L]$$

$$[H] = 2([S]^{-1} - [S]^{-1}[R][S]^{-1}).$$

The only difference compared with a single branch is, that in building $[Y_{AA}]$, $[Y_{AB}]$ in (13), a matrix $[S]^{-1}$ is entered instead of a scalar value. Also in each time step a vector $[I_{k,m}]$ enters into $[I_{\text{total}}]$ instead of a scalar value.

If Fig. 11 is part of a multiphase $\pi$-equivalent representing a line section, then each set of terminals will be capacitance connected. These capacitances are actually single branches; thus no new formula is necessary. BPA's program treats them as a matrix entity $[C]$ to speed up the solution.

*Lossless Multiphase Line*

Equation (1) is also valid for the multiphase line if the scalars are replaced by vectors $[e]$, $[i]$ and matrices $[L']$, $[C']$. By differentiating a second time, one of the vector variables can be eliminated, which gives

$$[\partial^2 e(x,t)/\partial x^2] = [L'][C'][\partial^2 e(x,t)/\partial t^2] \quad (18a)$$

$$[\partial^2 i(x,t)/\partial x^2] = [C'][L'][\partial^2 i(x,t)/\partial t^2]. \quad (18b)$$

The solution of (18) is complicated by the presence of off-diagonal elements in the matrices, which occur because of mutual couplings between the phases. This difficulty is overcome if the phase variables are transformed into mode variables by similarity transformations that produce diagonal matrices in the modal equations [2], [13], [14]. This is the well-known eigenvalue problem. Each of the independent equations in the modal domain can then be solved with the algorithm for the single-phase line by using its modal travel time and its modal surge impedance. The transformation matrices, which give the transition to the phase domain, will generally be different for voltages and currents, e.g.,

$$[e_{\text{phase}}] = [T_e][e_{\text{mode}}] \quad (19a)$$

$$[i_{\text{phase}}] = [T_i][i_{\text{mode}}]. \quad (19b)$$

The columns in $[T_e]$, $[T_i]$ are always undetermined by a constant factor, if not normalized. A helpful relation [2], [15] is:

$$[T_i]_{\text{unnormalized}} = [C'][T_e]. \quad (19c)$$

If all diagonal elements in $[L']$ are equal to $L'_{\text{self}}$ and all off-diagonal elements are equal to $L'_{\text{mutual}}$ (analogous for $[C']$), then a simple transformation is possible, even if the inductances are frequency dependent [15]:

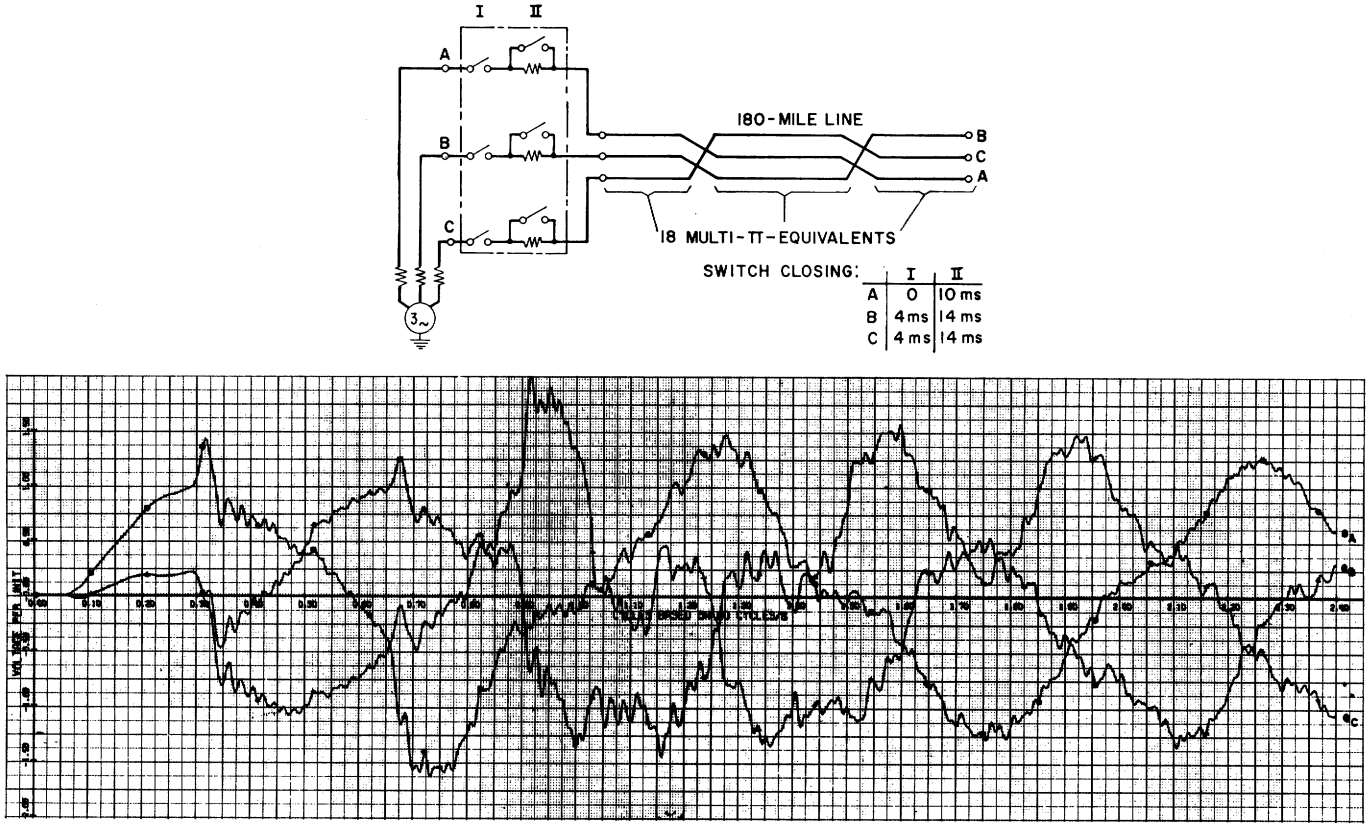


Fig. 12. Sequential closing. Network and results at the receiving end. Line energizing: 180-mile line, transposed at 60 and 120 miles. RLC for 60 Hz.

$$[T_e] = [T_i] = \begin{bmatrix} 1 & 1 & \cdots & 1 \\ 1 & 1-M & \cdots & 1 \\ \cdots & \cdots & \cdots & \cdots \\ 1 & 1 & \cdots & 1-M \end{bmatrix} \tag{20}$$

where $M$ is the number of phases.

It can be shown [2] that the phase current vector $[i_{k,m}]$ entering the nodes at terminal $k$ toward $m$ can again be written as a linear vector equation

$$[i_{k,m}(t)] = [G][e_k(t)] + [I_k] \tag{21}$$

and analogous for $[i_{m,k}]$. Equation (21) is derived from a set of modal equations, subjected to the transformations (19). In building $[Y_{AA}]$, $[Y_{AB}]$ in (13), a matrix $[G]$ is entered instead of a scalar value $1/Z$. The vector $[I_k]$, which enters $[I_A]$, is calculated from the past history of the modal quantities. Since the span $(t - \tau)$ for picking up the past is different for each mode, a time argument was deliberately omitted in writing $[I_k]$. Even though the nodal equations are in phase quantities, the past history must be recorded in modal quantities.

## IV. Frequency-Dependent Line Parameters

Skin effects in the earth return and conductors make the line parameters $R'$ and $L'$ frequency dependent [11], [14]. In multiphase lines, this affects primarily the mode associated with earth return. It is not easy to take the frequency dependence into account and at the same time maintain the generality of the program. Methods using the Fourier transform [15], [16] or the Laplace transform [17] are usually restricted to the case of a single line. Work is in progress at BPA to incorporate the frequency dependence approximately into the method of characteristics; then, instead of one value from the past history, several weighted samples will go into the computation of $I_k$ and $I_m$. The weights would have to be chosen to match the frequency spectrum derived from Carson's formula [11] or from measurements on the line. In a similar approach [18], the earth return mode is passed through two RC filters before entering the node, while the others are attenuated without distortion.

## V. Examples

Two simple cases are used to illustrate applications of the program. Fig. 12 shows the results for sequential closing of a three-phase, open-ended line. The curves were automatically plotted by a Calcomp plotter. For this study, the line was represented by 18 multi-$\pi$-equivalents with (coupled) lumped parameters. Fig. 13 shows the voltage at the receiving end of a single-phase line (320 miles long, $R' = 0.0376\ \Omega$/mi, $L' = 1.52$ mH/mi, $C' = 0.0143\ \mu$F/mi), that is terminated by an inductance of 0.1 H and excited with a step function $e(t) = 10$ V. The solid curve results from representing the line with 32 lumped-parameter equivalents, the dashed curve from a distributed-parameter representation.

## VI. Conclusions

A generalized digital computer method for solving transient phenomena in single- or multiphase systems has been described. The method is very efficient and capable of handling very large networks. Further work is necessary to find a satisfactory way to represent frequency dependence of line parameters.

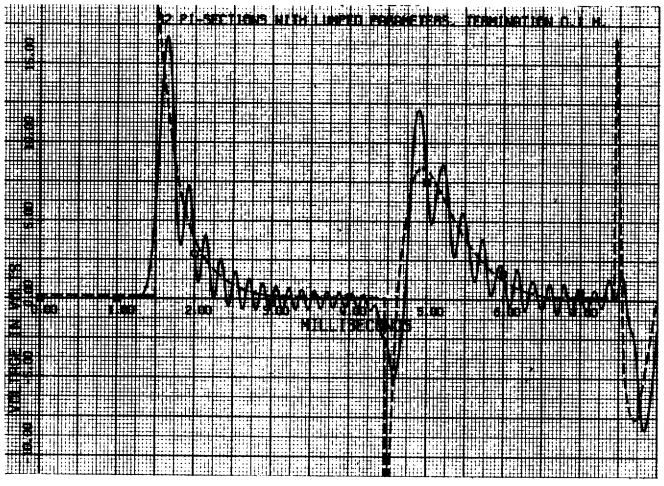

Fig. 13. Single-phase line with inductive termination.

## Appendix I

### Recording the Past History

The equivalent current sources $I$ in Figs. 1–3 constitute that part of the past history, known from preceding time steps, that has to be recorded and constantly updated. They are needed in building the vector $[I_{\text{total}}]$. For each inductance and capacitance a single value $I_{k,m}(t - \Delta t)$ must be recorded, for each lossless line a double list $I_k$, $I_m$ for the time steps $t - \Delta t$, $t - 2\Delta t$, $\ldots$, $t - \tau$.

In updating $I_{k,m}$ for inductances and capacitances, it is faster to use recursive formulas:

$$I_{k,m}(t - \Delta t) = \pm (I_{k,m}(t - 2\Delta t) + 2x)$$

(+ for inductance, − for capacitance), with $x = G(e_k(t - \Delta t) - e_m(t - \Delta t))$ and $G = \Delta t/2L$ for inductance and $G = 2C/\Delta t$ for capacitance.

These formulas are easily verified by expressing the currents in (9b) and (10b) by (9a) and (10a), respectively. To assure correct initial values in the very first time step, $I_{k,m}$ must be preset before entering the time step loop

$$I_{k,m}(\text{initial}) = i_{k,m}(0) - G(e_k(0) - e_m(0)).$$

The initial conditions $e(0)$ for voltages and $i(0)$ for currents are part of the input.

For a lossless line the values $I_k$, $I_m$ must be recorded for $t - \Delta t$, $t - 2\Delta t$, $\ldots$, back to $t - \tau$; they are stored in one double list, where the portion for each line has its length adjusted to its specific travel time $\tau$. After $[e(t)]$ has been found, the double list is first shifted back one time step (entries for $t - \Delta t$ become entries for $t - 2\Delta t$, etc.); then $I_k(t - \tau)$, $I_m(t - \tau)$ are computed and entered into the list. Physically, the list is not shifted; instead, the starting address is raised by 1 modulo {length of double list} [8]. The initial values for $I_k$, $I_m$ must be given for $t = 0, -\Delta t, -2\Delta t, \ldots, -\tau$. The necessity to know them beyond $t = 0$ is a consequence of recording the terminal conditions only. If the conditions were also given along the line at travel time increments $\Delta t$, then the initial values at $t = 0$ would suffice.

BPA's computer program has features that help to speed up the solution. Thus a series connection of resistance, inductance, and capacitance is treated as a single branch. This reduces the number of nodes; the respective formulas can be derived by eliminating the inner nodes in the connection [2]. Likewise, single- or multiphase $\pi$-equivalents with series $[R]$ and $[L]$ matrices and with identical shunt $[C]$ matrix at both terminals are treated as one element. If the system has identical network elements (e.g., in a chain of $\pi$-equivalents), then the data are specified and stored only once.

## Appendix II

### Initial Conditions

BPA's computer program has two options for setting nonzero initial conditions. Voltages and currents at any point in a study can be stored and used again as initial conditions in subsequent studies that take off from that point (usually with a different $\Delta t$). They can also be computed for any sinusoidal steady-state condition with a subroutine "multiphase steady-state solution." The first option must be used if the steady-state solution is nonsinusoidal because of nonlinearities. In this case a transient study is made once and for all over a long enough time span to settle to the steady state. This gives initial conditions for all subsequent studies.

### Acknowledgment

The author wants to thank his colleagues at the Bonneville Power Administration, notably Dr. A. Budner, J. W. Walker, and W. F. Tinney, for their help and for their encouragements. The idea of weighted samples to incorporate the frequency dependence of line parameters is due to Dr. A. Budner, and the subroutine to get ac steady-state initial conditions was written by J. W. Walker.

### References

[1] H. Prinz and H. Dommel, "Überspannungsberechnung in Hochspannungsnetzen," presented at the Sixth Meeting for Industrial Plant Managers, sponsored by Allianz Insurance Company, Munich, Germany, 1964.
[2] H. Dommel, "A method for solving transient phenomena in multiphase system," *Proc. 2nd Power System Computation Conference 1966* (Stockholm, Sweden), Rept. 5.8.
[3] F. H. Branin, Jr., "Computer methods of network analysis," *Proc. IEEE*, vol. 55, pp. 1787–1801, November 1967.
[4] L. Bergeron, *Du Coup de Belier en Hydraulique au Coup de Foudre en Electricité*. Paris: Dunod, 1949. Transl., *Water Hammer in Hydraulics and Wave Surges in Electricity* (Translating Committee sponsored by ASME). New York: Wiley, 1961.
[5] H. Prinz, W. Zaengl, and O. Völcker, "Das Bergeron-Verfahren zur Loesung von Wanderwellen," *Bull. SEV*, vol. 16, pp. 725–739, August 1962.
[6] W. Frey and P. Althammer, "Die Berechnung elektromagnetischer Ausgleichsvorgaenge auf Leitungen mit Hilfe eines Digitalrechners," *Brown Boveri Mitt.*, vol. 48, pp. 344–355, 1961.
[7] P. L. Arlett and R. Murray-Shelley, "An improved method for the calculation of transients on transmission lines using a digital computer," *Proc. PICA Conf.*, pp. 195–211, 1965.
[8] F. H. Branin, Jr., "Transient analysis of lossless transmission lines," *Proc. IEEE*, vol. 55, pp. 2012–2013, November 1967.
[9] L. O. Barthold and G. K. Carter, "Digital traveling-wave solutions," *AIEE Trans. (Power Apparatus and Systems)*, vol. 80, pp. 812–820, December 1961.
[10] W. F. Tinney and J. W. Walker, "Direct solutions of sparse network equations by optimally ordered triangular factorization," *Proc. IEEE*, vol. 55, pp. 1801–1809, November 1967.
[11] J. R. Carson, "Wave propagation in overhead wires with ground return," *Bell Syst. Tech. J.*, vol. 5, pp. 539–554, 1926.
[12] A. Ralston, *A First Course in Numerical Analysis*. New York: McGraw-Hill, 1965.
[13] A. J. McElroy and H. M. Smith, "Propagation of switching-surge wavefronts on EHV transmission lines," *AIEE Trans. (Power Apparatus and Systems)*, vol. 81, pp. 983–998, 1962 (February 1963 sec.).
[14] D. E. Hedman, "Propagation on overhead transmission lines I—theory of modal analysis," *IEEE Trans. Power Apparatus and Systems*, vol. PAS-84, pp. 200–211, March 1965; discussion, pp. 489–492, June 1965.

[15] H. Karrenbauer, "Ausbreitung von Wanderwellen bei verschiedenen Anordnungen von Freileitungen im Hinblick auf die Form der Einschwingspannung bei Abstandskurzschluessen," doctoral dissertation, Munich, Germany, 1967.
[16] M. J. Battisson, S. J. Day, N. Mullineux, K. C. Parton, and J. R. Reed, "Calculation of switching phenomena in power systems," *Proc. IEE* (London), vol. 114, pp. 478–486, April 1967; discussion, pp. 1457–1463, October 1967.
[17] R. Uram and R. W. Miller, "Mathematical analysis and solution of transmission-line transients I—theory," *IEEE Trans. Power Apparatus and Systems*, vol. 83, pp. 1116–1137, November 1964.
[18] A. I. Dolginov, A. I. Stupel', and S. L. Levina, "Algorithm and programme for a digital computer study of electromagnetic transients occurring in power system" (in Russian), *Elektrichestvo*, no. 8, pp. 23–29, 1966; English transl. in *Elec. Technol.* (USSR), vols. 2–3, pp. 376–393, 1966.

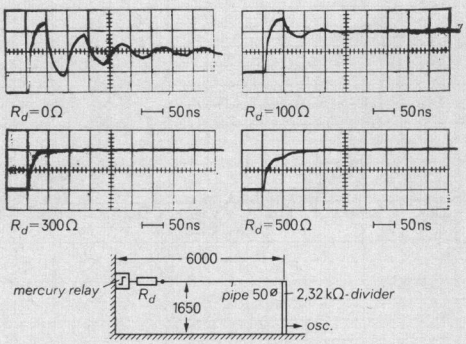


Fig. 14. Measured step response of a low-impedance voltage divider.

## Discussion

**W. Zaengl** and **F. W. Heilbronner** (Hochspannungsinstitut der Technischen Hochschule München, Munich, Germany): Dr. Dommel is to be congratulated for these lucid elaborations of the treatment of electromagnetic transients. In order to demonstrate how effective this method is, we wish to append two examples of a single-phase application of the algorithm as described and the verification by experiments: 1) evaluation of the step response of an impulse voltage measuring circuit and 2) computation of the voltage breakdown in sparkgaps.

1) In high-voltage measuring techniques voltage dividers are used which cannot be constructed coaxially and are, because of voltages up to some million volts, of big dimensions. Therefore the voltage to be measured is led to the divider by metallic pipes, at the input end of which, in general, a damping resistor is connected.

For this purpose the equivalent circuit of the total measuring circuit is best represented by a lossless line (for the metallic pipe), on which traveling wave phenomena occur, and lumped parameters (for damping resistor and voltage divider). An analytic general solution to get the step response of this network is not possible.

In Fig. 14 the used measuring circuit is sketched with its dimensions. The 2.32-kΩ divider consists of stacked resistors. The output voltage, reduced by a factor of 100, is measured by an oscilloscope (Tektronix 585). Four oscillograms of the output voltage are given, resulting from various damping resistors $R_d$, if a voltage step generated by a mercury relay occurs at the input end of the measuring circuit.

In Fig. 15 the equivalent circuit of the test setup with its data is given and the results of the digital computation of the step response $G(t)$ with the program outlined in the paper. The surge impedance $Z = 272$ ohms and the travel time $\tau = 20$ ns result from the geometric dimensions of the pipe. The divider is represented by a multisection network of a total of five $T$ quadripoles and an input shunt capacity $C_p = 5$ pF. In the calculation a step width $\Delta t$ of $2 \cdot 10^{-9}$ seconds was used. The comparison shows a very good agreement with the experimental results of Fig. 14.

2) Whereas the solution of the foregoing problem requires no specific modification of the straightforward procedure as described in the paper, in the case of voltage breakdown, nonlinearities have to be taken into account [19]. One means of evaluating the voltage $u$ at a time $t$ during breakdown of a gap was given by Toepler [20]:

$$u^{(t)} = k \cdot a \cdot i^{(t)} \Big/ \int_0^t i^{(t)}\, d\xi \qquad (22)$$

i.e., the resistance of the spark is inversely proportional to the amount of charge which has flowed into the gap ($a$ = gap spacing in cm, $k$ = constant in the range of $10^{-4}$ V·s/cm, $i^{(t)}$ = current in amperes, $t$ = time in seconds).

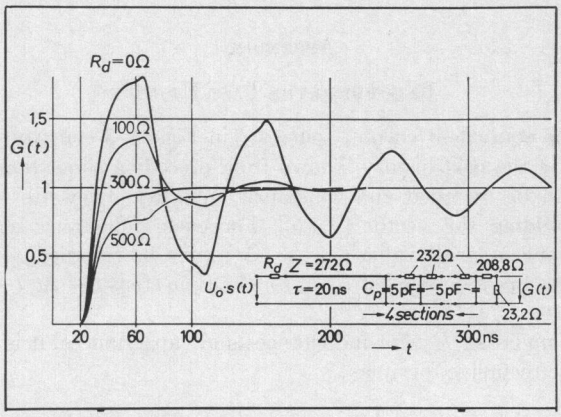


Fig. 15. Calculated step response of the test setup according to Fig. 14.

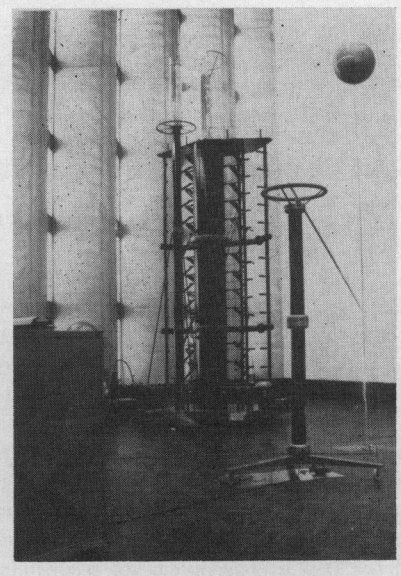

Fig. 16. Test setup. Front left: screened measuring cabin; front center: damped capacitive divider; front right: 80-cm rod–rod gap; center: 3-million-volt impulse generator (capacitive divider is used as load capacitance and is standing in front of the generator).

Manuscript received July 3, 1968.

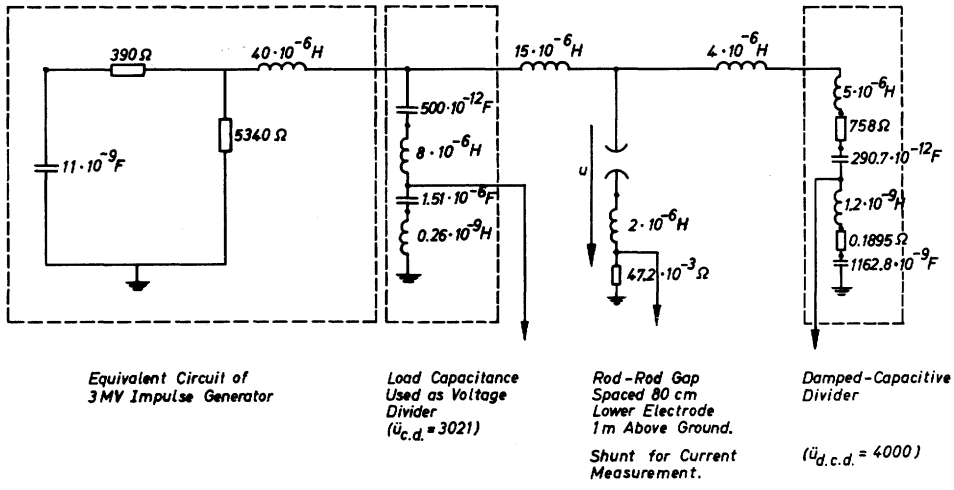


Fig. 17. Equivalent impulse circuit of Fig. 16.

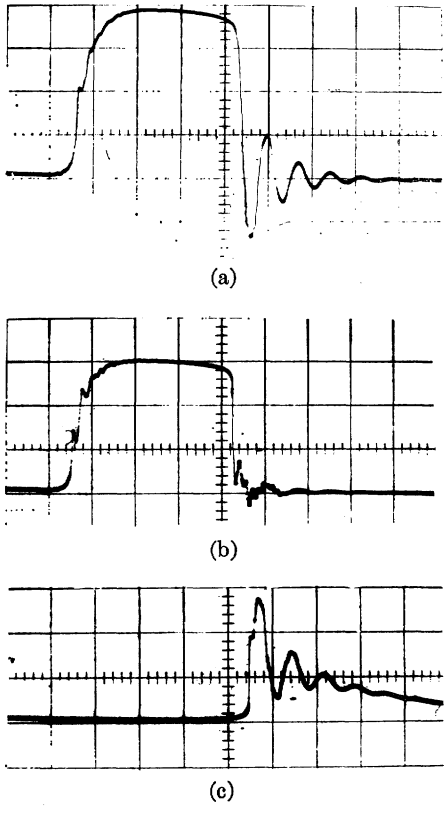


Fig. 18. Oscillograms from the voltage breakdown of a 80-cm rod–rod gap (temperature: 20°C, 716 mm Hg); horizontal deflection $10^{-6}$ seconds/division. (a) Capacitive divider: 138 kV per vertical division. (b) Damped capacitive divider: 183 kV per division. (c) Current shunt: 1060 amperes per vertical division.

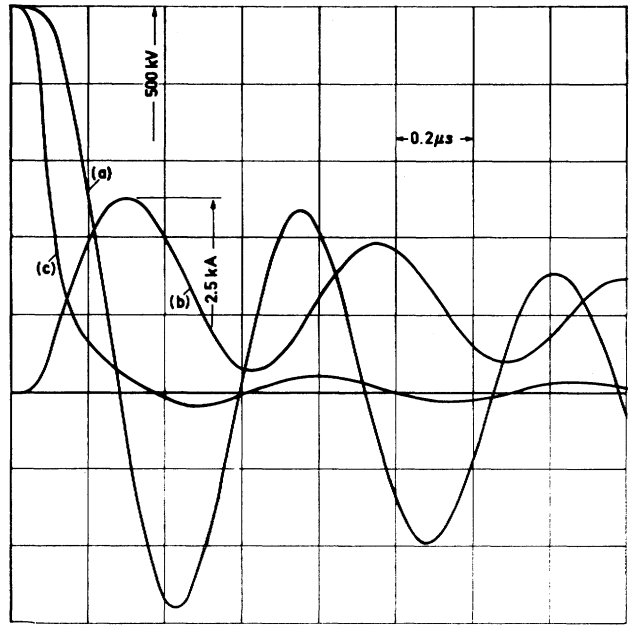


Fig. 19. Calculated voltages in different points and gap current at breakdown according to Fig. 17. (a)—voltage of capacitive divider; (b)—gap current $i^{(t)}$; (c)—gap voltage $u^{(t)}$.

Using the trapezoidal rule of integration, (22) can be rewritten as

$$u^{(t)} = \frac{k \cdot a \cdot i^{(t)}}{\text{int}^{(t-\Delta t)} + \frac{1}{2}(i^{(t-\Delta t)} + i^{(t)}) \cdot \Delta t} \tag{23}$$

where $\text{int}^{(t-\Delta t)}$ is the value of the integral in the denominator of (22) up to the time $(t - \Delta t)$. This is the equivalent expression of $f(i_{k,m}(t))$ in (16a). Since the solution in connection with (15) would be of the quadratic type, it was found sufficient to linearize the problem and take the resistance of the previous time step $(t - \Delta t)$:

$$R^{(t-\Delta t)} = \frac{k \cdot a}{\text{int}^{(t-2\Delta t)} + \frac{1}{2} \cdot (i^{(t-2\Delta t)} + i^{(t-\Delta t)}) \cdot \Delta t}. \tag{24}$$

Thus, in terms of the paper, the voltage across a sparkgap between the nodes $k$ and $m$ will be

$$u^{(t)} = \frac{R^{(t-\Delta t)} \cdot (e_k(t) - e_m(t))^{(\text{linear})}}{R^{(t-\Delta t)} + (z_{k,k} - z_{k,m} - z_{m,k} + z_{m,m})}. \tag{25}$$

In order to start the process, in (24) a certain initial value of $\text{int}^{(t-\Delta_2 t)}$ is needed. This means in physical terms, that by some predischarges the gap must have been ionized and thus assumed some conductivity. Experience has shown that for a start the value of $R^{(t-\Delta t)}$ might be chosen a thousand times higher than the biggest resistance in the circuit.

As a demonstration, in Fig. 18 three oscillograms (Tektronix 507) of the breakdown of a 80-cm rod–rod gap in the test circuit of Figs. 16 and 17 are given. The calculated values with $k = 0.3 \cdot 10^{-4}$ V·s/cm and $\Delta t = 20 \cdot 10^{-9}$ seconds, multiplied by the corresponding divider ratios, are plotted in Fig. 19. They correspond fairly well to the oscillograms. The voltage resulting from the damped capacitive divider is within $\pm 1$ percent of $u$ and is therefore not plotted.

Two conclusions may be drawn from a comparison of Figs. 18 and 19 and are stated without further explanation: 1) A damped capacitive divider [21] reflects the gap voltage much better than a purely capacitive divider, and 2) the common equivalent circuit of a divider may be too rough in the cases where higher harmonics occur. Then an equivalent circuit as in item 1) would be necessary.

The described application of the transient algorithm in high-voltage impulse circuits has led the discussers to various secondary problems and suggestions, of which two can be sketched here in general terms only.

1) In problems with many nodes, computer storage might be too small for building up the matrix $[Y]$. Thus the method of diacoptics is of help, especially when two major parts of the circuit are connected by a single lead which can be represented by a lumped parameter (inductance in Fig. 17).

2) If sudden changes of network parameters occur, e.g., the breakdown of a sparkgap on account of a certain overvoltage, where the resistance changes from the order of megohm to ohm in fifty to some hundred nanoseconds, it might be desirable to make the time step $\Delta t$ smaller and increase it again when the rate of change is no longer of importance. Thus it is necessary to adapt the stepwidth $\Delta t$ to the rate of voltage change in the network.

## References

[19] F. Heilbronner and H. Kärner, "Ein Verfahren zur digitalen Berechnung des Spannungszusammenbruchs von Funkenstrecken," *ETZ-A*, vol. 89, pp. 101–108, 1968.
[20] M. Toepler, "Funkenkonstante, Zündfunken und Wanderwelle," *Arch. f. Elektrotech.*, vol. 16, pp. 305–316, 1925.
[21] W. Zaengl, "Das Messen hoher, rasch veränderlicher Stossspannungen," doctoral dissertation, Munich, 1964.

**D. G. Taylor** and **M. R. Payne** (Central Electricity Generating Board, London, England): We have also programmed the Bergeron method for single-phase switching problems and are currently engaged in extending the treatment to multiconductor systems. Lumped $L$ and shunt $C$ have been represented as short lines and special "hyper-nodes" have been introduced to deal with series $R$ and series $C$. Only one past history is stored which necessitates subdividing lines into sections of equal traveling time. Processed system data together with past and present values of voltage and current are stored in a structured file (in core) which is passed, using list-processing techniques, in order to advance the solution by one time step.

One advantage of subdividing lines over storing multiple past histories is that series resistance can be introduced between all sections; we have found this to be desirable in cases where the response is oscillatory and the degree of attenuation is important. The author's comments on this point would be appreciated.

A source of approximation which should be mentioned arises from the necessity for all traveling times to be integral multiples of the time increment $\Delta t$. This also applies to the method of multiple past histories since any interpolation between values is invalid. The problem is made more severe in multiconductor systems by the propagation velocities in the modes being different, in some cases by small but significant amounts. How does the author take this into account in making his initial choice of time increment, in particular for systems including asymmetrical multiconductor configurations?

In conclusion the author is to be congratulated on his adaptation of the problem for use with ordered-elimination techniques which have already made such an impact on steady-state analysis. We look forward to the author's further developments in this field, particularly with regard to the treatment of frequency dependence.

Manuscript received July 3, 1968.

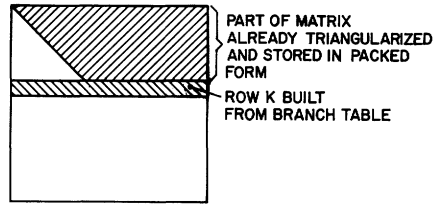


Fig. 20. Triangularization scheme.

**H. W. Dommel**: The author wants to thank Dr. W. Zaengl, Mr. F. W. Heilbronner, Mr. D. G. Taylor, and Mr. M. R. Payne for their valuable discussions, which illustrate the usefulness of Bergeron's method in traveling wave studies and also raise some interesting questions.

One of the main differences between the author's computer program and that of Mr. D. G. Taylor and Mr. M. R. Payne is the subdivision of the line into sections of travel time $\tau = \Delta t$ in the latter. It appears that considerable savings in computer time (but not in storage requirements) are possible when such subdivisions are avoided and multiple past histories are stored. It must be admitted, however, that lumped series resistances can be included more easily in more places with the line being subdivided, even though this can always be done with the author's program in the definition of the model at the expense of more input data. Interestingly enough, test examples showed very little or no difference at all between the insertion of lumped series resistances in few or many places (section *Approximation of Series Resistance of Lines*). Therefore, the automatic insertion at three places (terminals and midpoint) was felt to be adequate. This observation might not be true for all cases. Also, not too much significance has been placed on the approximation of distributed resistance by lumped series resistances in developing the program, since the final objective has been the approximation of the frequency dependence in the zero-sequence mode. This has not been included yet, but preliminary tests with a weighting function representation look promising.

Mr. D. G. Taylor and Mr. M. R. Payne use a stub-line (short line) representation for lumped (series and shunt) $L$ and shunt $C$. It can be shown that this stub-line representation for shunt $L$ and shunt $C$ is equivalent with the integration of (8b), and the respective equation for $C$, by the trapezoidal rule over two time steps from $t - 2\Delta t$ to $t$ (no such simple equivalence was found for series $L$). Since the author's method for lumped $L$ and $C$ is based on the trapezoidal rule of integration over one time step only from $t - \Delta t$ to $t$, it is more accurate than stub lines. The stub-line representation is very helpful, however, in studies involving more than one nonlinear element. As described in the section *Nonlinear and Time-Varying Parameters*, more than one nonlinear element can be handled in closed form only if they are separated by elements of finite travel time. A stub-line representation accomplishes just such a separation. As an example, a case involving a lightning arrester connected to a nonlinear inductance (transformer with saturation) can be solved by modeling the total inductance as a linear and nonlinear inductance in series, with the linear inductance placed on the side of the lightning arrester and treated as a stub line.

Mr. D. G. Taylor and Mr. M. R. Payne raise the question of errors introduced either by making all travel times an integral multiple of $\Delta t$ or by using interpolation between past values. It is true that this question is even more critical in multiconductor systems with small differences in mode propagation velocities. Interpolation is indeed questionable if sudden changes occur. However, the presence of inductances and capacitances often, though not always, smoothes out sudden changes; then interpolation is a good and valid approximation. Sudden changes may also be introduced through stub-line representations and not lie in the nature of the problem. In cases where sudden changes do occur, the user has an option in which all travel times are rounded to the nearest integral multiple of $\Delta t$. As of now, the step width $\Delta t$ must be chosen by the user.

In the first part of their discussion, Dr. W. Zaengl and Mr. F. W. Heilbronner show how closely computed results can agree with test results. This speaks at least as much for their good engineering

Manuscript received August 8, 1968.

judgment in selecting an equivalent model as it does for the usefulness of the computer program. Their effort to include the dynamic law of spark gaps into the program should be of interest to high-voltage engineers.

As to the specific questions raised, it is felt that the sparsity technique used (optimally ordered elimination with packed storage of nonzero elements only) is more efficient than the method of diacoptics. It was probably not made clear in the paper that the matrix $[Y]$ is never built explicitly. Rather, a branch table is used to store the information for the matrix $[Y]$. As indicated in Fig. 20 for the $k$th elimination step, the original row $k$ is built from a search of the branch table (therefore, only one working row is necessary), then the elements to the left of the diagonal are eliminated with the information contained in the already available rows $1, \cdots, k-1$ of the triangularized matrix, and finally the elements $Y'_{k,k}, Y'_{k,k+1}, \cdots$ of this transformed row are added in packed form to the triangularized matrix. In a way, the method does have a built-in tearing feature similar to diacoptics in cases involving lines with distributed parameters, which disconnect the network topologically. This disconnection is more than tearing in diacoptics, since it is a true disconnection where no reconnection effect has to be introduced at a later stage of the algorithm. Thus, the use of a stub-line representation for the inductance in Fig. 17 with surge impedance $Z = L/\Delta t$ and travel time $\tau = \Delta t$, might reduce the storage requirements beyond those already achieved through sparsity. The possibility to change $\Delta t$ during the computation would indeed be desirable. It is a straightforward programming task, involving changes of $[Y]$. Due to lack of time, it has not been incorporated so far.

# Nonlinear Programming Solutions for Load-Flow, Minimum-Loss, and Economic Dispatching Problems

ALBERT M. SASSON, MEMBER, IEEE

*Abstract*—**A unified approach to load-flow, minimum-loss, and economic dispatching problems is presented. A load-flow solution is shown to coincide with the minimum of a function of the power system equations. An unconstrained minimization method, developed by Fletcher–Powell, is used to solve the load-flow probl.m. The method always finds a solution or indicates the nonexistence of a solution. Its performance is highly independent of the reference-slack bus position and requires no acceleration factors. Several constrained minimization techniques that solve the minimum-loss and economic dispatching problems are investigated. These include the Fiacco–McCormick, Lootsma, and Zangwill methods. The technique finally recommended is shown to be an extension of the method used to solve the load-flow problem. The approved IEEE test systems, and other systems whose response to conventional methods was known, have been solved.**

## Introduction

MUCH WORK has been done in the fields of load-flow analysis and economic dispatching; some papers have presented methods that obtain a minimum-loss solution. Each of these problems has been solved independently from the others. The methods discussed in this paper present a unified approach which demonstrates that all three problems fall into a single class of optimization problems.

Paper 68 TP 673–PWR, recommended and approved by the Power System Engineering Committee of the IEEE Power Group for presentation at the IEEE Summer Power Meeting, Chicago, Ill., June 23–28, 1968. Manuscript submitted February 7, 1968; made available for printing May 14, 1968.

The author is with the Imperial College of Science and Technology, London, England, and the Instituto Tecnologico y de Estudios Superiores de Monterrey, Monterrey, N. L., Mexico.

The load-flow problem [1], [2] was first solved by a simplified Newton–Raphson approach which involved the power system nodal admittance matrix. As the equations are not quadratic, the simplified approach together with an iterative process was justified. Later [3] an iterative Gauss–Seidel approach was successfully used. Further improvements were based on using the nodal impedance matrix [4] and the mesh impedance matrix [5]. More recently Newton's technique has been used [6], [7] claiming extremely rapid convergence. Even if much progress has been made in load-flow analysis, there are situations which cause difficulties in obtaining solutions with some of these methods. The position of the reference-slack bus, the choice of acceleration factors, the existence of negative line reactances, a large ratio of long-to-short line reactance for lines terminating in the same bus, and certain types of radial systems are the cause of much instability in methods of solution of the load-flow problem. When a divergent solution is obtained, it is not clear whether the divergence has been due to instability in the method used or to the fact that there may not be a solution at all. The methods presented in this paper are quite insensitive to many of the factors which cause instability to existing methods and give a definite answer as to whether a solution exists or not. The approach is based on the construction of a function of the power-system equations, whose minimum coincides with the solution of the equations.

The minimum-loss problem has also been solved in various ways. The first approach to the problem was to solve the economic dispatching problem minimizing losses at the same time. This ignored the possibility of minimizing losses by an optimal use of the reactive capabilities of the system as a whole. It is from the second point of view that this paper considers the minimum-loss problem. One of the first attempts [8] was to